

This is a post-peer-review, pre-copyedit version of an article published in Luo, W., et al. *Higher capability of C₃ than C₄ plants to use nitrogen inferred from nitrogen stable isotopes along an aridity gradient* in Plant and soil, vol. 428, issue 1-2 (Jul. 2018), p. 93-103. The final authenticated version is available online at DOI [10.1007/s11104-018-3661-2](https://doi.org/10.1007/s11104-018-3661-2)

Cop. All rights reserved.

1 **Higher capability of C3 than C4 plants to use nitrogen inferred from nitrogen**
2 **stable isotopes along an aridity gradient**

3 Wentao Luo¹, Xiaoguang Wang^{1,2}, Jordi Sardans^{3,4}, Zhengwen Wang¹, Feike A.

4 Dijkstra⁵, Xiao-Tao Lü^{1*}, Josep Peñuelas^{3,4}, Xingguo Han¹

5 *¹Erguna Forest-Steppe Ecotone Research Station, Institute of Applied Ecology,*

6 *Chinese Academy of Sciences, Shenyang110164, China;*

7 *²College of Environment and Resources, Dalian Minzu University, Dalian 116600,*

8 *China;*

9 *³CSIC, Global Ecology Unit CREAM-CSIC-UAB, Bellaterra, 08193 Catalonia, Spain;*

10 *⁴CREAF, Cerdanyola del Vallès, 08193 Catalonia, Spain;*

11 *⁵Sydney Institute of Agriculture, School of Life and Environmental Sciences, The*

12 *University of Sydney, NSW, 2006, Australia;*

13 **Author for correspondence: Dr. Xiao-Tao Lü;*

14 *E-mail: lvxiaotao@iae.ac.cn; Tel: +86(24)83970752*

15

16 **Abstract**

17 *Background and Aims* The nitrogen isotope composition ($\delta^{15}\text{N}$) of plants in arid and
18 semiarid grasslands is affected by environmental factors, especially water availability.
19 Nevertheless, it is unclear whether the response of $\delta^{15}\text{N}$ to water availability differs
20 between C3 and C4 photosynthetic pathways.

21 *Methods* We investigated plant $\delta^{15}\text{N}$ of coexisting C3 and C4 species as a function of
22 aridity along a 3200 km aridity gradient across the arid and semi-arid grasslands of
23 northern China.

24 *Results* Aridity was positively correlated with plant $\delta^{15}\text{N}$ values in both C3 and C4
25 plants and also in the entire plant community, whereas soil bulk $\delta^{15}\text{N}$ values increased
26 first and then decreased along the aridity gradient. The N uptake by C4 plants
27 appeared to be more affected by competition pressure of neighboring plants and soil
28 microbes than for C3 plants along the transect.

29 *Conclusions* The decoupled relationship between plant and soil $\delta^{15}\text{N}$ values indicated
30 that variations in vegetation and soil $\delta^{15}\text{N}$ values were driven by differential
31 biogeochemical processes, while different soil N sources were used for plant growth
32 along the climatic gradient. The advantage of C3 plants in the use of N may
33 counteract the competitive advantage that C4 plants have over C3 plants due to their
34 higher water use efficiency under drier conditions. These findings can help understand
35 why C4 plants do not completely replace C3 plants in drier environments despite their
36 higher water use efficiency.

37 **Keywords**

38 Competition, grassland transect, photosynthetic pathway, precipitation, trade-off.

39 **Introduction**

40 The relative proportions of the stable isotopes of nitrogen (^{14}N and ^{15}N , expressed as
41 $\delta^{15}\text{N}$) in ecosystem components can serve as a proxy of N dynamics and as a
42 nondestructive indicator of how plants respond to environmental changes in terrestrial
43 ecosystems (Amundson et al. 2003; Díaz et al. 2016; Robinson 2001). The two stable
44 isotopes of N are discriminated in several fundamental biogeochemical processes that
45 in turn are sensitive to environmental conditions (Amundson et al. 2003; Robinson
46 2001), so $\delta^{15}\text{N}$ values have been widely used to reflect how environmental changes
47 alter the ecosystem N-cycles over large scales (Craine et al. 2009; Ogaya and
48 Peñuelas 2008; Peri et al. 2012; Swap et al. 2004).

49 The values of $\delta^{15}\text{N}$ in individual plants are determined by the isotopic ratio of the
50 external source and the redistribution of N within the plant (Evans 2001; Kolb and
51 Evans 2002), while plant community-level $\delta^{15}\text{N}$ values are also controlled by the
52 relative abundance of plant species (Craine et al. 2015; Peri et al. 2012). Previous
53 studies have shown different $\delta^{15}\text{N}$ values between C3 and C4 photosynthetic
54 pathways (Brown 1978; Sage and Percy 1987a; b). For instance, higher $\delta^{15}\text{N}$ values
55 in C4 plants than their C3 neighbors were found in western Australia (Wooller et al.
56 2005) and the Mediterranean region (Hartman and Danin 2010), but C3 plants had
57 higher $\delta^{15}\text{N}$ values than C4 plants in southern Africa (Aranibar et al. 2008).

58 Relationships between plant $\delta^{15}\text{N}$ values and precipitation are a product of water
59 availability and soil N sources during plant growth (Handley et al. 1999). The general
60 pattern that soil and plant $\delta^{15}\text{N}$ values decrease with increased precipitation has been

61 demonstrated at both regional and global scales and suggests different biogeochemical
62 processes and cycles of N induced by increased aridity, producing more open cycles
63 in drier regions (Amundson et al. 2003; Aranibar et al. 2004; Craine et al. 2009;
64 Ogaya and Peñuelas 2008). In less stressed environments the higher plant uptake
65 allows for a greater N retention in the plant-soil system and reduced loss of ^{15}N in a
66 more closed N cycle (Amundson et al. 2003; Aranibar et al. 2004). However, the
67 responses of plant $\delta^{15}\text{N}$ to environmental changes are also dependent on the
68 photosynthetic pathways (Murphy and Bowman 2009). The response of plant $\delta^{15}\text{N}$
69 values to increasing water availability was more positive in C3 than in C4 grasses in
70 Australian grasslands (Murphy and Bowman 2009). It has been argued that plant $\delta^{15}\text{N}$
71 values are inversely correlated with precipitation for C3 but not for C4 plants in
72 southern Africa (Swap et al. 2004).

73 The differential responses of $\delta^{15}\text{N}$ values between the coexisting C3 and C4 plants
74 to climate changes are caused by their different N sources (Wang et al. 2016;
75 Michelsen et al. 1998; Pardo et al. 2006). It has been well known that the N sources
76 from mycorrhizal fungi and direct root uptake from soils can vary isotopically as a
77 result of local environmental conditions (Hobbie et al. 2000). The enhanced
78 dependence of C3 or C4 plants on mycorrhizal fungi generally reduces their
79 corresponding $\delta^{15}\text{N}$ values by delivering ^{15}N -depleted N to host plants (Hobbie and
80 Colpaert 2003; Hobbie and Högberg 2012), and C3 or C4 plants that prefer nitrate are
81 predicted to have lower $\delta^{15}\text{N}$ values than those plants that prefer ammonium (Houlton
82 et al. 2007). Moreover, changes in soil water availability may also alter $\delta^{15}\text{N}$ values in

83 C3 and C4 plants by changing their rooting depth and N availability with soil depth
84 and thereby the ^{15}N signature of plant N sources (Kahmen et al. 2008), because nitrate
85 and ammonium sources at different soil depths can vary in $\delta^{15}\text{N}$ signature (Hobbie
86 and Ouimette 2009; Xue et al. 2009). Until recently, however, a lack of available
87 ecological data has limited our ability to determine the underlying mechanisms for the
88 differential responses of C3 and C4 photosynthetic pathways to climatic variables
89 (Hartman and Danin 2010).

90 To address this knowledge gap, we investigated plant $\delta^{15}\text{N}$ of all the species in 26
91 plant communities across a 3200 km climatic gradient in arid and semiarid grasslands
92 of northern China, a suitable study region because the impact of climatic factors on
93 ecosystem N cycles is particularly strong as water stress and N availability are the
94 main constraints limiting plant growth and microbial activity in these areas (Bai et al.
95 2004; Cai et al. 2017). The C3 and C4 species are widely distributed and coexist
96 across this transect. The dominant plant growth forms gradually changed from grasses
97 and forbs to low shrubs with increasing aridity from the east to the west (Hilbig 1995;
98 Ni 2003; Pyankov et al. 2000). The unique features of this region encompass
99 relatively gentle geographical relief, distinct patterns of precipitation and temperature,
100 and relatively low N deposition levels. We hypothesized that I) plant $\delta^{15}\text{N}$ values
101 would increase towards the dry end of the climatic gradient for both C3 and C4 plants
102 and the whole plant community, and II) the response sensitivity would differ between
103 the coexisting C3 and C4 plants given the differences in N metabolism and the large
104 fractionations within plants (Robinson 2001). Specifically, we expected that C3 plants

105 would be more sensitive to aridity than C4 plants, consistent with previous results in
106 southern Africa (Swap et al. 2004) and Australian grasslands (Murphy and Bowman
107 2009).

108 **Material and Methods**

109 **Study sites**

110 In early August 2012, our study was conducted along an east-west transect across arid
111 and semiarid grasslands in northern China, which has been previously described
112 (Wang et al. 2014; Luo et al. 2016). This transect is approximately 3200 km long and
113 covers approximately 10° latitude and 33° longitude (39.8-50.5°N and 87.7-120.5°E)
114 (Figure 1). The topography of the study area consists of gently rolling hills and
115 tablelands, with elevations ranging from 700 m in the east to 1500 m above sea level
116 in the west. The arid and semiarid grasslands are far from human perturbations,
117 subjected to minimal animal grazing and other anthropogenic disturbances. This
118 region has a dry, continental climate with marked annual variation in both temperature
119 and precipitation. Mean annual precipitation (MAP) ranges from 450 mm (east) to 50
120 (west) mm, and mean annual temperature (MAT) ranges from -1.5°C (east) to 9.5°C
121 (west). The interaction of increasing MAP and decreasing MAT is closely tracked by
122 species richness and vegetation cover (%), which both increase with increased water
123 availability from the west to the east across this transect. A total of 26 sites at intervals
124 of *ca.* 150 km were selected along the transect. The latitude, longitude and elevation
125 of each sampling site were recorded by GPS (eTrex Venture, Garmin, USA).

126 Four representative types of vegetation can be found along the transect: desert

127 steppe, typical steppe and meadow steppe, which are characterized by increasing
128 precipitation and decreasing temperature from the west to the east (Figure 1). The
129 desert steppe, at the dry end of the gradient, is dominated by low shrubs *Calligonum*
130 *mongolicum* (C3) and *Suaeda microphylla* (C4), with low species richness and soil
131 organic matter content. The typical steppe, in the central part of the gradient, is
132 dominated by *Salsola collina* (C4) and *Reaumuria soongarica* (C3). The meadow
133 steppe, at the wet end of the gradient, is dominated by *Leymus chinensis* (C3), *Stipa*
134 *grandis* (C3) and *Cleistogenes squarrosa* (C4) and has relatively high species richness
135 and soil organic matter content. Related soil types of this region are gray-brown desert
136 soils, brown calcic soils and chestnut soils distributed from west to east, belonging to
137 the Kastanozems in the classification system of the Food and Agriculture
138 Organization and Mollisol order of the US Soil Taxonomy.

139 **Sampling and measurement**

140 At each site, two 50 m × 50 m main plots were established and five 1 m × 1 m
141 sampling subplots (or 5 m × 5 m sampling subplots in site dominated by low shrub)
142 were placed within each main plot at the four corners and the center (Figure 1). Plant
143 species presence were measured in each subplots, and from these data species
144 richness (number of plant species per subplot) were calculated. Standing crop was
145 estimated from the dry biomass of the aboveground living parts. Aboveground
146 biomass was sampled by clipping all plants at ground level within each sampling
147 subplot. All living plants were sorted to species and then stored in paper bags. Plant
148 materials were dried at 105 °C for 30 min in a portable drying oven to minimize

149 respiration and decomposition and were later completely oven dried at 65°C to
150 constant weight in the laboratory. After removal of surface litter, one composite soil
151 sample (0-10 cm depth) was randomly collected from each sampling subplot using a
152 soil corer (2.5 cm diameter). Soil samples was carefully removed from the plant
153 material and then separated into two sub-samples: one was stored in a cloth bag at
154 room temperature (air-dried soils); the other one was stored in a plastic bag in a
155 refrigerator at 4°C (fresh soils). A detailed description of the vegetation and soil
156 survey was documented in Luo et al. (2015; 2016).

157 Dried plant and soil materials were ground in a ball mill (NM200, Retsch, Haan,
158 Germany) and stored in a plastic bag until further analysis. Plant and soil bulk $\delta^{15}\text{N}$
159 values and soil total N concentrations were determined using an elemental analyzer
160 (Elementar Vario Micro Cube, Elementar, Germany) connected to an isotope ratio
161 mass spectrometer (IsoPrime100, Isoprime Ltd., UK), with an overall precision
162 better than 0.2‰. $\delta^{15}\text{N}$ values are expressed in per mil (‰) unit, relative to the
163 atmospheric N_2 standards.

164 Methods for the determination of soil pH and microbial-biomass N (MBN) has
165 been described previously (Luo et al. 2016). Briefly, soil pH was measured using a pH
166 electrode (S210 SevenCompact™, Mettler, Germany) in a 1: 2.5 mixture of soil:
167 water. The concentration of MBN was measured with the fumigation-extraction
168 method.

169 The MAT and MAP data (data range 1950-2000) were extracted from a global
170 climate dataset with a resolution of $0.0083^\circ \times 0.0083^\circ$ (approximately 1 km² at the

171 equator), obtained from <http://www.worldclim.org>. The potential evapotranspiration
172 (PET) data (data range 1950-2000) were extracted from the CGIAR-CSI Global
173 Aridity Index and Global Potential Evapo-Transpiration Climate Database
174 (<http://www.cgiar-csi.org/data/global-aridity-and-pet-database>). Aridity (unitless) was
175 calculated as 1-AI, where AI, the ratio of MAP to PET, is the aridity index (Luo et al.
176 2016). Aridity therefore increased with increasing MAT and decreasing MAP. Across
177 this transect, aridity ranged from 0.45 to 0.95, equivalent to a range in MAP of 450-50
178 mm, and a range in MAT ranged from -1.5 to 9.5 °C. The aridity was applied to
179 incorporate MAP and MAT into one parameter to assess the variations in plant $\delta^{15}\text{N}$
180 values along the climatic gradient due to the strongly positive correlation between
181 PET and MAT.

182 **Data analysis**

183 All sampled plant species were classified into C3 or C4 photosynthetic pathways. If
184 the specimen could be assigned to a genus, classification was made using the
185 identification in Watson and Dallwitz (1992). If the specimen could not be identified
186 to generic level, classification was made by the $\delta^{13}\text{C}$ values (Cerling et al. 1997).

187 Plant community $\delta^{15}\text{N}$ values were defined as the overall mean of $\delta^{15}\text{N}$ values
188 across all species (n, species richness) weighted by the relative (fractional)
189 contribution of each species to the overall biomass at each quadrat (Kichenin et al.
190 2013):

191 Community $\delta^{15}\text{N} = (\text{biomass}_1 \times \delta^{15}\text{N}_1 + \text{biomass}_2 \times \delta^{15}\text{N}_2 + \dots + \text{biomass}_n \times \delta^{15}\text{N}_n) / \text{total}$
192 biomass.

193 Ordinary least squares (OLS) regression was used to analyze the responses of plant

194 community $\delta^{15}\text{N}$ values to increasing aridity. Binary regression was conducted to
195 analyze the relationship between aridity and soil $\delta^{15}\text{N}$ values. Then, OLS regression
196 was also used to examine the correlation between mean community and soil $\delta^{15}\text{N}$
197 values. To further analyze patterns of plant $\delta^{15}\text{N}$ values, OLS regression was applied
198 to test the relationships of plant $\delta^{15}\text{N}$ values and N concentrations with aridity for both
199 C3 and C4 plants. Then, OLS regression was applied to test the relationships of plant
200 $\delta^{15}\text{N}$ values with species richness for both C3 and C4 plants. We conducted analysis
201 of covariance to identify the differences in the slopes of the regression lines between
202 C3 and C4 photosynthetic pathways. Steeper slope means greater sensitivity of $\delta^{15}\text{N}$
203 value in this plant type in response to aridity.

204 To examine the underlying mechanism under the different responses of $\delta^{15}\text{N}$ values
205 to aridity between coexisting C3 and C4 plants, structural equation modeling (SEM)
206 was applied to examine the interactive effects of climatic and soil variables on the
207 $\delta^{15}\text{N}$ values in C3 and C4 plants, respectively. In the SEM analysis, we compared the
208 model-implied variance-covariance matrix against the observed variance-covariance
209 matrix. Data were fitted to the models using the Akaike information criterion and the
210 goodness of fit index. For simplicity, the least significant path was deleted and the
211 model was re-estimated; then the next least significant path was removed, and so on,
212 until the paths that remained in the final SEM were all significant. Standard errors and
213 the significance level (P value) were calculated using bootstrapping (1200
214 repetitions).

215 All statistical analyses were carried out using the statistical package of SPSS 13.0

216 for Windows® (SPSS Inc., Chicago, IL, USA, 2004) and the *sem* function in the *sem*
217 package of R-project (R i386 3.1.1).

218 **Results**

219 Plant $\delta^{15}\text{N}$ values significantly increased with increasing aridity at the community
220 level ($P < 0.001$, Figure 2). Removing the leguminous species from this analysis did
221 not change the results (data not shown). The relative biomass of leguminous species
222 (%) showed no significant relationship with aridity (data not shown). Plant
223 communities in drier sites contained a greater percentage of total plant biomass of
224 species with higher $\delta^{15}\text{N}$ values (Table 1). Soil $\delta^{15}\text{N}$ values increased first and then
225 reduced with increasing aridity (Figure S1) and was nonlinearly associated with plant
226 community $\delta^{15}\text{N}$ values (Figure 3). Removing three sites with soil $\delta^{15}\text{N}$ values > 10 ‰
227 (outliers) did not change the results (see the insets in Figures 3 and S1).

228 Plant $\delta^{15}\text{N}$ values also significantly increased with aridity in both C3 and C4 plants
229 at the level of individual species ($P < 0.001$, Figure 4). The interaction between aridity
230 and type of photosynthetic pathway was significant, *i.e.*, the slope of the regression
231 line for aridity and $\delta^{15}\text{N}$ values was significantly steeper for C4 than C3 plants
232 ($P < 0.001$). When the specific-biomass weighting factor was considered, the response
233 of $\delta^{15}\text{N}$ values to increasing aridity was also more positive in the C4 than in the C3
234 plant group (Figure S2). Plant N content did not show any significant relationships
235 with aridity for both C3 and C4 plants along the transect (Figure S3). Plant $\delta^{15}\text{N}$
236 values reduced with increasing species richness in both C3 and C4 plants, and the
237 slope of the regression line for species richness and $\delta^{15}\text{N}$ values was significantly

238 steeper for C4 than C3 plants ($P < 0.001$, Figure S4). The proportional contribution of
239 C3 plants to total biomass reduced and that of C4 plants increased with the increase in
240 aridity (Figure S5). Soil pH increased with increasing aridity, while standing crop,
241 species richness, soil total N concentration, soil C:N ratio, and MBN concentration all
242 reduced with increasing aridity along the transect (Figure S6).

243 The SEM analyses showed that the total effects of aridity, soil pH and ANPP were
244 positive on $\delta^{15}\text{N}$ values in both C3 (Figure 5a) and C4 plants (Figure 5b). Aridity
245 indirectly affected plant $\delta^{15}\text{N}$ values via the positive effect on soil pH and the negative
246 effects on ANPP and species richness for both C3 (Figure 5a) and C4 plants (Figure
247 5b). The total effects of soil total N and MBN concentrations were negatively and
248 positively correlated with $\delta^{15}\text{N}$ values in C4 plants, respectively (Figure 5b). Aridity
249 indirectly affected plant $\delta^{15}\text{N}$ values via the negative effects on soil total N and MBN
250 concentrations for C4 plants (Figure 5b).

251

252 **Discussion**

253 **N stable isotopes in plants along the aridity gradient**

254 Consistent with our hypothesis, plant $\delta^{15}\text{N}$ values of both the C3 and C4 functional
255 groups and the entire community increased towards the dry end of the climatic
256 gradient across northern China's grasslands, where N and water availability are two of
257 the most constraining factors limiting plant growth and microbial activity. This
258 finding is similar to that reported in other continents (Aranibar et al. 2008; Austin and
259 Sala 1999; Heaton 1987; Swap et al. 2004) and in an extensive global synthesis
260 (McCulley et al. 2009; Murphy and Bowman 2009; Schulze et al. 1998) conducted at
261 the level of species rather than the entire plant community. Plant $\delta^{15}\text{N}$ values also
262 increased with aridity in our study in the entire plant community, similar to individual
263 species, which was due to the substitution of plant species/functional groups with
264 lower $\delta^{15}\text{N}$ by those with higher $\delta^{15}\text{N}$ when aridity rose along the climatic gradient
265 (see Table 1). Higher plant $\delta^{15}\text{N}$ values indicate a lower capacity of plants to retain N,
266 because the lighter ^{14}N isotope is more easily cycled and lost (Dalal et al. 2013;
267 McCulley et al. 2009). Plant species that are less efficient in retaining N are favored
268 when aridity increases along the climatic gradient. This result suggests that water
269 conservative mechanisms constitute a trade off with the capacity to retain and use N.
270 This trade-off has been observed and commented in previous studies (Dijkstra et al.
271 2016). Thus, the biological response to drier conditions when water limitation is the
272 main driver of adaptive responses provokes a decrease in the capacity to retain N in
273 the plant community.

274 The increased plant $\delta^{15}\text{N}$ values with aridity, however, do not agree with our
275 previous study along the same gradient, which found that the ecosystem N-cycles,
276 based on soil bulk $\delta^{15}\text{N}$ rather than plant $\delta^{15}\text{N}$ signals, were more closed at the two
277 ends of the aridity gradient and more open in the middle of the aridity gradient (Wang
278 et al. 2014). Similarly, Díaz et al. (2016) recently reported that soil $\delta^{15}\text{N}$ values
279 increased with increasing aridity along an elevational/climatic gradient in northern
280 Chile, as expected, whereas plant $\delta^{15}\text{N}$ values had a hump-shaped relationship with
281 increasing aridity. The decoupled relationship between the $\delta^{15}\text{N}$ values of plants and
282 soils indicates the differences in biogeochemical processes underlying N dynamics
283 between vegetation and soil. An increase in plant $\delta^{15}\text{N}$ values with aridity,
284 independent of soil bulk $\delta^{15}\text{N}$ values, may be caused by changes in the uptake of
285 nitrate versus ammonium along the aridity gradient (Houlton et al. 2007; Takebayashi
286 et al. 2010). Species that prefer nitrate relative to ammonium generally have lower
287 $\delta^{15}\text{N}$ values than species that prefer ammonium (Houlton et al. 2007). In our previous
288 study along the same climatic gradient, we found that $\delta^{15}\text{N}$ values of ammonium
289 consistently increased, while $\delta^{15}\text{N}$ values of nitrate increased first and then decreased
290 with increasing aridity (see Liu et al. 2017). These results suggest a shift of dominant
291 inorganic N sources for plants with aridity, resulting in a positive relationship between
292 aridity and plant $\delta^{15}\text{N}$ values and a decoupled relationship between plant and soil bulk
293 $\delta^{15}\text{N}$ values. Similarly, Houlton et al. (2007) demonstrated that increased aridity
294 resulted in a switch in the dominant N source for plant growth, leading to a reduction
295 in plant $\delta^{15}\text{N}$ values from drier to wetter sites in tropical forest ecosystems.

296 **N isotope and N use in C4 versus C3 plants**

297 In line with our hypothesis, the responses of plant $\delta^{15}\text{N}$ values to environmental
298 changes differed between the coexisting C3 and C4 photosynthetic pathways (Figures
299 5 and 6). The $\delta^{15}\text{N}$ values in C4 plants were positively correlated with soil MBN
300 concentration and negatively correlated with soil total N concentration but not in C3
301 plants (Figure 5). This suggests a stronger competition intensity of N uptake between
302 soil microbes and C4 plants when soil N content becomes scarcer under drier
303 conditions (Liu et al. 2016; Ouyang et al. 2016). The increases in plant $\delta^{15}\text{N}$ values in
304 C4 plants along the aridity gradient therefore corresponded to a large proportion of
305 soil N incorporated into microbial biomass, suggesting that C4 plants competed with
306 soil microbes for N less strongly than C3 plants (Liu et al. 2016; Ouyang et al. 2016)).
307 Moreover, our results showed that the reduction in species richness with increasing
308 aridity directly resulted in a reduction in plant $\delta^{15}\text{N}$ values in both C3 and C4 plants,
309 with the effects being stronger in C4 than C3 plants (Figure S4). These results suggest
310 that C4 plants were more sensitive to plant neighborhood competition with respect to
311 N uptake than C3 plants (Harrison et al. 2007; Mariotte et al. 2013). Taken together,
312 C4 plants appeared more affected by competition pressure of neighboring plants and
313 soil microbes than C3 plants with respect to N uptake and C3 plants had an apparent
314 advantage in the use and retention of N compared to C4 plants in arid and semiarid
315 grasslands.

316 This advantage of C3 plants in the use of N may improve their competitive ability
317 and thus their survival capacity under dry conditions. Previous studies have reported

318 that C3 plants would be replaced by C4 plants due to their lower water-use efficiency
319 if the global climate becomes drier in the near future (Pyankov et al. 2000; Wittmer et
320 al. 2010). However, this higher N-use efficiency we observed in C3 plants could
321 counteract the competitive advantage of the more water-use efficient C4 plants under
322 drier conditions, thereby partially avoiding the total replacement of C3 by C4 plants.
323 A reduction in transpiration can further decrease the capacity of C4 plants to take up
324 and compete for nutrients (Cramer et al. 2009). Our results provide new evidence of a
325 trade-off between N-use and water-use efficiencies for plants with different
326 photosynthetic pathways (Dijkstra et al. 2016). The higher ability of C3 plants to
327 absorb, retain and use N could, at least partially, explain why C3 plants are not fully
328 replaced by the more water-use efficient C4 plants under arid conditions when N
329 supply decreases.

330 **Conclusion**

331 Our results have two important implications for predicting the responses of vegetation
332 and biogeochemical cycles to climate change. First, plant $\delta^{15}\text{N}$ values of both the C3
333 and C4 functional groups and the entire community increased towards drier
334 conditions due to an increase in $\delta^{15}\text{N}$ of each individual species, and also to an
335 increased dominance of species with higher $\delta^{15}\text{N}$ values. Along the aridity gradient,
336 plant $\delta^{15}\text{N}$ values did not covary with soil bulk $\delta^{15}\text{N}$ values, resulting from a shift in
337 dominant inorganic N sources for plant growth along the aridity gradient. The
338 decoupled relationships suggest that the mechanisms underlying soil bulk $\delta^{15}\text{N}$
339 patterns should be carefully applied to plant $\delta^{15}\text{N}$ patterns in arid and semiarid

340 ecosystems. Second, our results suggest that competition pressure for N by
341 neighboring plants and soil microbes became more intense for C4 than C3 plants,
342 thereby partly counteracting the competitive advantage of C4 plants due to their
343 higher water use efficiencies under drier and warmer conditions. These findings
344 provide new hypotheses to explain why C3 plants are not completely replaced by C4
345 plants in drier and warmer conditions.

346 **Acknowledgments**

347 We thank all members of the Field Expedition Team from the Institute of Applied
348 Ecology, Chinese Academy of Sciences, for assistance with the collection of the field
349 data. We thank three anonymous referees as well as the Handling Editor for
350 constructive comments on the manuscript. This work was supported by the National
351 Basic Research Program of China (2016YFC0500601, 2016YFC0500700 and
352 2015CB150802), National Natural Science Foundation of China (41600302,
353 3231470505 and 41273094), Strategic Priority Research Program of the Chinese
354 Academy of Sciences (XDB15010403), Youth Innovation Promotion Association
355 CAS (2014174), and the Key Research Program from CAS (KFZD-SW-305-002). JP
356 and JS were funded by the European Research Council Synergy grant ERC-SyG-
357 2013-610028, IMBALANCE-P, the Spanish Government grant CGL2013-48074-P
358 and the Catalan Government grant SGR 2014-274.

359

360 **References**

- 361 Amundson R, Austin AT, Schuur EAG, Yoo K, Matzek V, Kendall C, Uebersax A,
362 Brenner D, Baisden WT (2003) Global patterns of the isotopic composition of
363 soil and plant nitrogen. *Glob Biogeochem Cy* 17: 1031.
364 doi:10.1029/2002GB001903.
- 365 Aranibar JN, Anderson IC, Epstein HE, Feral CJW, Swap RJ, Ramontsho J, Macko
366 SA (2008) Nitrogen isotope composition of soils, C3 and C4 plants along land
367 use gradients in southern Africa. *J Arid Environ* 72: 326-337.
- 368 Aranibar JN, Otter L, Macko SA, Feral CJW, Epstein HE, Dowty PR, Eckardt F,
369 Shugart HH, Swap RJ (2004) Nitrogen cycling in the soil-plant system along a
370 precipitation gradient in the Kalahari sands. *Glob Chang Biol* 10: 359-373.
- 371 Austin AT, Sala OE (1999) Foliar $\delta^{15}\text{N}$ is negatively correlated with rainfall along the
372 IGBP transect in Australia. *Aust J Plant Physiol* 26: 293-295.
- 373 Bai Y, Han X, Wu J, Chen Z, Li L (2004) Ecosystem stability and compensatory
374 effects in the Inner Mongolia grassland. *Nature* 431: 181-184.
- 375 Brown R (1978) A difference in N use efficiency in C3 and C4 plants and its
376 implications in adaptation and evolution. *Crop Sci* 18: 93-98.
- 377 Cai J, Weiner J, Wang R, Luo W, Zhang Y, Liu H, Xu Z, Li H, Zhang Y, Jiang Y
378 (2017) Effects of nitrogen and water addition on trace element stoichiometry
379 in five grassland species. *J Plant Res* 4: 659-668.
- 380 Cerling TE, Harris JM, MacFadden BJ, Leakey MG, Quade J, Eisenmann V,
381 Ehleringer JR (1997) Global vegetation change through the Miocene/Pliocene

382 boundary. *Nature* 389: 153-158.

383 Craine JM, Brookshire ENJ, Cramer MD, Hasselquist NJ, Koba K, Marin-Spiotta E,
384 Wang L (2015) Ecological interpretations of nitrogen isotope ratios of
385 terrestrial plants and soils. *Plant Soil* 396: 1-26.

386 Craine JM, Elmore AJ, Aidar MPM, Bustamante M, Dawson TE, Hobbie EA,
387 Kahmen A, Mack MC, McLauchlan KK, Michelsen A, Nardoto GB, Pardo
388 LH, Peñuelas J, Reich PB, Schuur EAG, Stock WD, Templer PH, Virginia RA,
389 Welker JM, Wright IJ (2009) Global patterns of foliar nitrogen isotopes and
390 their relationships with climate, mycorrhizal fungi, foliar nutrient
391 concentrations, and nitrogen availability. *New Phytol* 183: 980-992.

392 Cramer MD, Hawkins HJ, Verboom GA (2009) The importance of nutritional
393 regulation of plant water flux. *Oecologia* 161: 15-24.

394 Dalal RC, Strong WM, Cooper JE, King AJ (2013) Relationship between water use
395 and nitrogen use efficiency discerned by ^{13}C discrimination and ^{15}N isotope
396 ratio in bread wheat grown under no-till. *Soil Till Res* 128: 110-118.

397 Díaz FP, Frugone M, Gutiérrez RA, Latorre C (2016) Nitrogen cycling in an extreme
398 hyperarid environment inferred from $\delta^{15}\text{N}$ analyses of plants, soils and
399 herbivore diet. *Sci Rep* 6, 22226. doi: 10.1038/srep22226

400 Dijkstra FA, Carrillo Y, Aspinwall MJ, Maier C, Canarini A, Tahaei H, Choat B,
401 Tissue DT (2016) Water, nitrogen and phosphorus use efficiencies of four tree
402 species in response to variable water and nutrient supply. *Plant Soil* 406: 187-
403 199.

404 Evans RD (2001) Physiological mechanisms influencing plant nitrogen isotope
405 composition. *Trends Plant Sci* 6: 121-126.

406 Handley LL, Austin AT, Robinson D, Scrimgeour CM, Raven JA, Heaton THE,
407 Schmidt S, Stewart GR (1999) The ^{15}N natural abundance ($\delta^{15}\text{N}$) of ecosystem
408 samples reflects measures of water availability. *Aust J Plant Physiol* 26: 185-
409 199.

410 Harrison KA, Bol R, Bardgett RD (2007) Preferences for different nitrogen forms by
411 coexisting plant species and soil microbes. *Ecology* 88: 989-999.

412 Hartman G, Danin A (2010) Isotopic values of plants in relation to water availability
413 in the Eastern Mediterranean region. *Oecologia* 162: 837-852.

414 Heaton TH (1987) The $^{15}\text{N}/^{14}\text{N}$ ratios of plants in South Africa and Namibia:
415 relationship to climate and coastal/saline environments. *Oecologia* 74: 236-
416 246.

417 Hilbig W (1995) *Vegetation of Mongolia*. SPB Academic Publishing.

418 Hobbie EA, Colpaert JV (2003) Nitrogen availability and colonization by mycorrhizal
419 fungi correlate with nitrogen isotope patterns in plants. *New Phytol* 157: 115-
420 126.

421 Hobbie EA, Högberg P (2012) Nitrogen isotopes link mycorrhizal fungi and plants to
422 nitrogen dynamics. *New Phytol* 196: 367-382.

423 Hobbie EA, Macko SA, Williams M (2000) Correlations between foliar $\delta^{15}\text{N}$ and
424 nitrogen concentrations may indicate plant-mycorrhizal interactions.
425 *Oecologia* 122: 273-283.

426 Hobbie EA, Ouimette AP (2009) Controls of nitrogen isotope patterns in soil profiles.
427 *Biogeochemistry* 95: 355-371.

428 Houlton BZ, Sigman DM, Schuur EA, Hedin LO (2007) A climate-driven switch in
429 plant nitrogen acquisition within tropical forest communities. *P Natl Acade Sci*
430 USA 104: 8902-8906.

431 Kahmen A, Wanek W, Buchmann N (2008) Foliar $\delta^{15}\text{N}$ values characterize soil N
432 cycling and reflect nitrate or ammonium preference of plants along a
433 temperate grassland gradient. *Oecologia* 156: 861-870.

434 Kichenin E, Wardle DA, Peltzer DA, Morse CW, Freschet GT (2013) Contrasting
435 effects of plant inter- and intraspecific variation on community-level trait
436 measures along an environmental gradient. *Funct Ecol* 27: 1254-1261.

437 Kolb K, Evans R (2002) Implications of leaf nitrogen recycling on the nitrogen
438 isotope composition of deciduous plant tissues. *New Phytol* 156: 57-64.

439 Liu D, Zhu W, Wang X, Pan Y, Wang C, Xi D, Bai E, Wang Y, Han X, Fang Y (2017)
440 Abiotic versus biotic controls on soil nitrogen cycling in drylands along a
441 3200km transect. *Biogeosciences* 14: 989-1001.

442 Liu Q, Qiao N, Xu X, Xin X, Han JY, Tian Y, Ouyang H, Kuzyakov Y (2016)
443 Nitrogen acquisition by plants and microorganisms in a temperate grassland.
444 *Sci Rep* 6: 22642. doi: 10.1038/srep22642.

445 Luo W, Elser JJ, Lü XT, Wang Z, Bai E, Yan C, Wang C, Li MH, Zimmermann NE,
446 Han X (2015) Plant nutrients do not covary with soil nutrients under changing
447 climatic conditions. *Glob Biogeochem Cy* 29: 1298-1308.

448 Luo W, Sardans J, Dijkstra FA, Peñuelas J, Lü XT, Wu H, Li MH, Bai E, Wang Z,
449 Han X, Jiang Y (2016) Thresholds in decoupled soil-plant elements under
450 changing climatic conditions. *Plant Soil* 409: 159-173.

451 Mariotte P, Vandenberghe C, Kardol P, Hagedorn F, Buttler A (2013) Subordinate
452 plant species enhance community resistance against drought in semi-natural
453 grasslands. *J Ecol* 101: 763-773.

454 McCulley RL, Burke IC, Lauenroth WK (2009) Conservation of nitrogen increases
455 with precipitation across a major grassland gradient in the Central Great Plains
456 of North America. *Oecologia* 159: 571-581.

457 Michelsen A, Quarmby C, Sleep D, Jonasson S (1998) Vascular plant ^{15}N natural
458 abundance in heath and forest tundra ecosystems is closely correlated with
459 presence and type of mycorrhizal fungi in roots. *Oecologia* 115: 406-418.

460 Murphy BP, Bowman D (2009) The carbon and nitrogen isotope composition of
461 Australian grasses in relation to climate. *Funct Ecol* 23: 1040-1049.

462 Ni J (2003) Plant functional types and climate along a precipitation gradient in
463 temperate grasslands, north-east China and south-east Mongolia. *J Arid
464 Environ* 53: 501-516.

465 Ogaya R, Peñuelas J (2008) Changes in leaf $\delta^{13}\text{C}$ and $\delta^{15}\text{N}$ for three Mediterranean
466 tree species in relation to soil water availability. *Acta Oecol* 34: 331-338.

467 Ouyang S, Tian Y, Liu Q, Zhang L, Wang R, Xu X (2016) Nitrogen competition
468 between three dominant plant species and microbes in a temperate grassland.
469 *Plant Soil* 408: 121-132.

470 Pardo L, Templer P, Goodale C, Duke S, Groffman P, Adams M, Boeckx P, Boggs J,
471 Campbell J, Colman B (2006) Regional Assessment of N Saturation using
472 Foliar and Root $\delta^{15}\text{N}$. *Biogeochemistry* 80: 143-171.

473 Peri PL, Ladd B, Pepper DA, Bonser SP, Laffan SW, Amelung W (2012) Carbon
474 ($\delta^{13}\text{C}$) and nitrogen ($\delta^{15}\text{N}$) stable isotope composition in plant and soil in
475 Southern Patagonia's native forests. *Glob Chang Biol* 18: 311-321.

476 Pyankov VI, Gunin PD, Tsoog S, Black CC (2000) C₄ plants in the vegetation of
477 Mongolia: their natural occurrence and geographical distribution in relation to
478 climate. *Oecologia* 123: 15-31.

479 Robinson D (2001) $\delta^{15}\text{N}$ as an integrator of the nitrogen cycle. *Trends Ecol Evol* 16:
480 153-162.

481 Sage RF, Percy RW (1987a) The nitrogen use efficiency of C₃ and C₄ plants I. Leaf
482 nitrogen, growth, and biomass partitioning in *Chenopodium album* (L.) and
483 *Amaranthus retroflexus* (L.). *Plant Physiol* 84: 954-958.

484 Sage RF, Percy RW (1987b) The nitrogen use efficiency of C₃ and C₄ plants II. Leaf
485 nitrogen effects on the gas exchange characteristics of *Chenopodium album*
486 (L.) and *Amaranthus retroflexus* (L.). *Plant Physiol* 84: 959-963.

487 Schulze ED, Williams RJ, Farquhar GD, Schulze W, Langridge J, Miller JM, Walker
488 BH (1998) Carbon and nitrogen isotope discrimination and nitrogen nutrition
489 of trees along a rainfall gradient in northern Australia. *Aust J Plant Physiol* 25:
490 413-425.

491 Swap RJ, Aranibar JN, Dowty PR, Gilhooly WP, Macko SA (2004) Natural

492 abundance of ^{13}C and ^{15}N in C_3 and C_4 vegetation of southern Africa: patterns
493 and implications. *Glob Chang Biol* 10: 350-358.

494 Takebayashi Y, Koba K, Sasaki Y, Fang Y, Yoh M (2010) The natural abundance of
495 ^{15}N in plant and soil-available N indicates a shift of main plant N resources to
496 NO_3^- from NH_4^+ along the N leaching gradient. *Rapid Commun Mass Sp* 24:
497 1001-1008.

498 Wang C, Wang X, Liu D, Wu H, Lu X, Fang Y, Cheng W, Luo W, Jiang P, Shi J, Yin
499 H, Zhou J, Han X, Bai E (2014) Aridity threshold in controlling ecosystem
500 nitrogen cycling in arid and semi-arid grasslands. *Nat Commun* 5: 499. doi:
501 10.1038/ncomms5799.

502 Wang R, Tian Y, Ouyang S, Xu X, Xu F, Zhang Y (2016) Nitrogen acquisition
503 strategies used by *Leymus chinensis* and *Stipa grandis* in temperate steppes.
504 *Biol Fert Soils* 52: 951-961.

505 Watson L, Dallwitz MJ (1992) Grass genera of the world: descriptions, illustrations,
506 identification, and information retrieval; including synonyms, morphology,
507 anatomy, physiology, phytochemistry, cytology, classification, pathogens,
508 world and local distribution, and references. [http://delta-](http://delta-intkey.com/grass/www/index.htm)
509 [intkey.com/grass/www/index.htm](http://delta-intkey.com/grass/www/index.htm).

510 Wittmer MH, Auerswald K, Bai Y, Schaeufele R, Schnyder H (2010) Changes in the
511 abundance of C_3/C_4 species of Inner Mongolia grassland: evidence from
512 isotopic composition of soil and vegetation. *Glob Chang Biol* 16: 605-616.

513 Wooller MJ, Johnson BJ, Wilkie A, Fogel ML (2005) Stable isotope characteristics

514 across narrow savanna/woodland ecotones in Wolfe Creek Meteorite Crater,
515 Western Australia. *Oecologia* 145: 100-112.

516 Xue D, Botte J, De Baets B, Accoe F, Nestler A, Taylor P, Van Cleemput O, Berglund
517 M, Boeckx P (2009) Present limitations and future prospects of stable isotope
518 methods for nitrate source identification in surface-and groundwater. *Water*
519 *Res* 43: 1159-1170.

520 **Table 1** The most abundant species of each community type. The mean N isotopic signature ($\delta^{15}\text{N}$) of the species along the gradient and the
 521 percentage of total individual plant biomass that the species represents in the corresponding community are indicated in parentheses in red and
 522 black, respectively.

Most abundance species in each community type								
Meadow steppe (low aridity)			Typical steppe (medium aridity)			Desert steppe (high aridity)		
<i>Achnatherum sibiricum</i>	0.69‰	4.10%	<i>Allium mongolicum</i>	2.14‰	2.57%	<i>Nitraria tangutorum</i>	3.13‰	14.40%
<i>Agropyron cristatum</i>	1.75‰	4.80%	<i>Allium polyrhizum</i>	4.17‰	2.90%	<i>Reaumuria songarica</i>	1.99‰	31.70%
<i>Allium bidentatum</i>	2.14‰	1.90%	<i>Allium ramosum</i>	2.95‰	0.15%	<i>Salsola passerina</i>	5.44‰	13.50%
<i>Allium mongolicum</i>	2.88‰	1.10%	<i>Allium spp.</i>	5.33‰	0.08%	<i>Suaeda microphylla</i>	5.81‰	11.50%
<i>Allium ramosum</i>	2.95‰	0.93%	<i>Allium tenuissimum</i>	1.74‰	0.08%	<i>Calligonum mongolicum</i>	5.84‰	3.80%
<i>Allium tenuissimum</i>	1.74‰	1.86%	<i>Artemisia scoparia</i>	1.86‰	0.46%	<i>Eragrostis pilosa</i>	2.59‰	4.80%
<i>Artemisia frigida</i>	2.28‰	3.43%	<i>Artemisia spp.</i>	1.24‰	0.15%			
<i>Asparagus cochinchinensis</i>	2.50‰	1.40%	<i>Cleistogenes spp.</i>	1.85‰	5.30%			
<i>Carex korshinskii</i>	0.89‰	4.98%	<i>Cleistogenes squarrosa</i>	0.46‰	3.60%			
<i>Chenopodium aristatum</i>	1.61‰	3.11%	<i>Eragrostis pilosa</i>	2.59‰	5.30%			
<i>Chenopodium glaucum</i>	4.66‰	2.80%	<i>Reaumuria songarica</i>	1.99‰	5.36%			
<i>Cleistogenes squarrosa</i>	0.46‰	10.1%	<i>Kochia prostrata</i>	5.75‰	3.57%			
<i>Kochia prostrata</i>	5.75‰	2.49%	<i>Salsola collina</i>	4.61‰	7.70%			
<i>Leymus chinensis</i>	1.26‰	9.35%	<i>Calligonum mongolicum</i>	5.44‰	5.60%			
<i>Potentilla acaulis</i>	0.99‰	0.93%	<i>Oxytropis aciphylla</i>	2.28‰	16%			
<i>Potentilla tanacetifolia</i>	0.25‰	1.86%	<i>Corispermum mongolicum</i>	5.84‰	2.60%			
<i>Salsola collina</i>	4.61‰	7.17%	<i>Caragana stenophylla</i>	0.33‰	2.09%			

Serratula centauroides 0.34‰ 7.62‰
Stipa spp. 2.27‰ 7.62‰

Represents 71% of total plant biomass in typical grasslands, with a weighted average of $\delta^{15}\text{N} = 1.38\text{‰}$

Represents 77% of total plant biomass in desert grasslands, with a weighted average of $\delta^{15}\text{N} = 2.75\text{‰}$

Represents 80% of total plant biomass in shrublands, with a weighted average of $\delta^{15}\text{N} = 6.01\text{‰}$

524 **Figure captions**

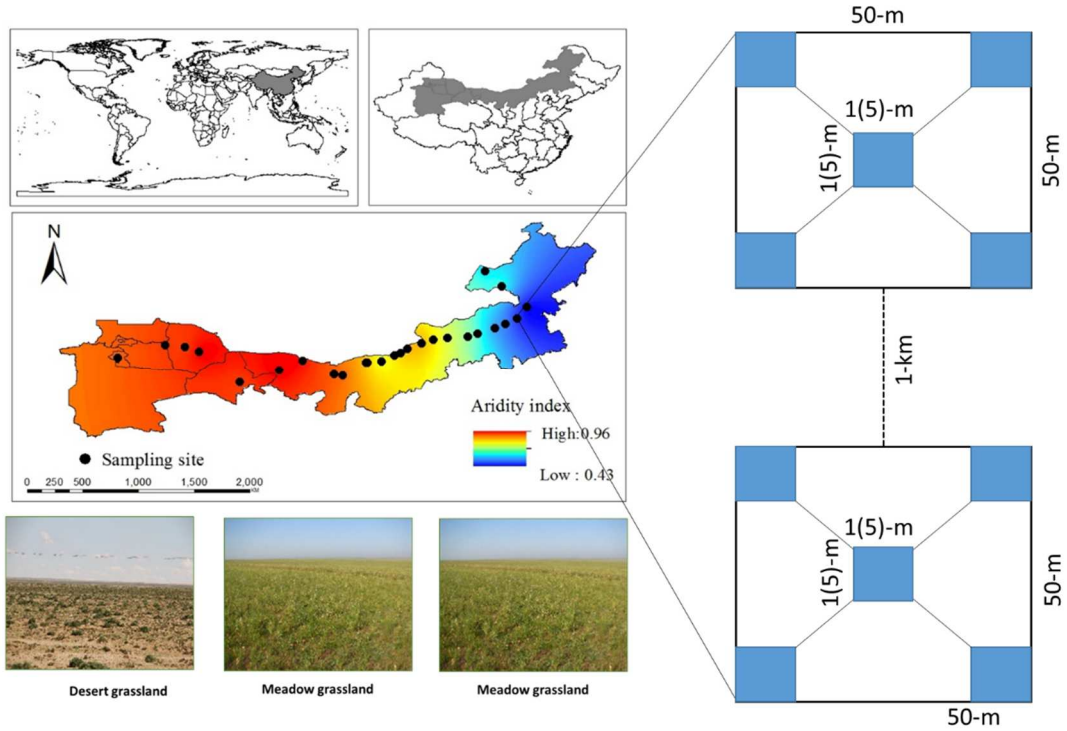
525 **Figure 1** A 3200-km long transect in arid and semiarid grasslands of northern China. A
526 total of 26 sampling sites from west to east were selected along the aridity gradient.
527 Two 50 m × 50 m plots were selected at each site, and five 1 m × 1 m sampling subplots
528 (or 5 m × 5 m sampling subplots in site dominated by low shrubs) were placed within
529 each plot. Three typical vegetation types are distributed with increasing aridity:
530 meadow steppe, typical steppe, and desert steppe. The dominant plant growth forms
531 change gradually from perennial grasses (*Leymus chinensis* (C3), *Stipa grandis* (C3)
532 and *Cleistogenes squarrosa* (C4)) to low shrubs (*Calligonum mongolicum* (C3) and
533 *Suaeda microphylla* (C4)).

534 **Figure 2** Correlation between aridity and plant community N isotopic signature
535 ($\delta^{15}\text{N}$) along the grassland transect in northern China. Plant community $\delta^{15}\text{N}$ values
536 were defined as the overall mean of $\delta^{15}\text{N}$ values across all species weighted by the
537 relative contribution of each species to the overall biomass. Aridity was calculated as
538 $1-\text{AI}$, where AI, the ratio of precipitation to potential evapotranspiration, is the aridity
539 index.

540 **Figure 3** Relationships between plant community and soil bulk $\delta^{15}\text{N}$ along the
541 grassland transect in northern China. Plant community $\delta^{15}\text{N}$ values were defined as
542 the overall mean of $\delta^{15}\text{N}$ values across all species weighted by the relative
543 contribution of each species to the overall biomass. When the three sites with soil
544 $\delta^{15}\text{N}$ values higher than 10 ‰ were removed, the non-linear relationship remained
545 between plant and soil $\delta^{15}\text{N}$ values.

546 **Figure 4** Correlation between aridity and N isotopic signature ($\delta^{15}\text{N}$) for C3 and C4
547 plants along the grassland transect in northern China. Aridity was calculated as 1-AI,
548 where AI, the ratio of precipitation to potential evapotranspiration, is the aridity index.

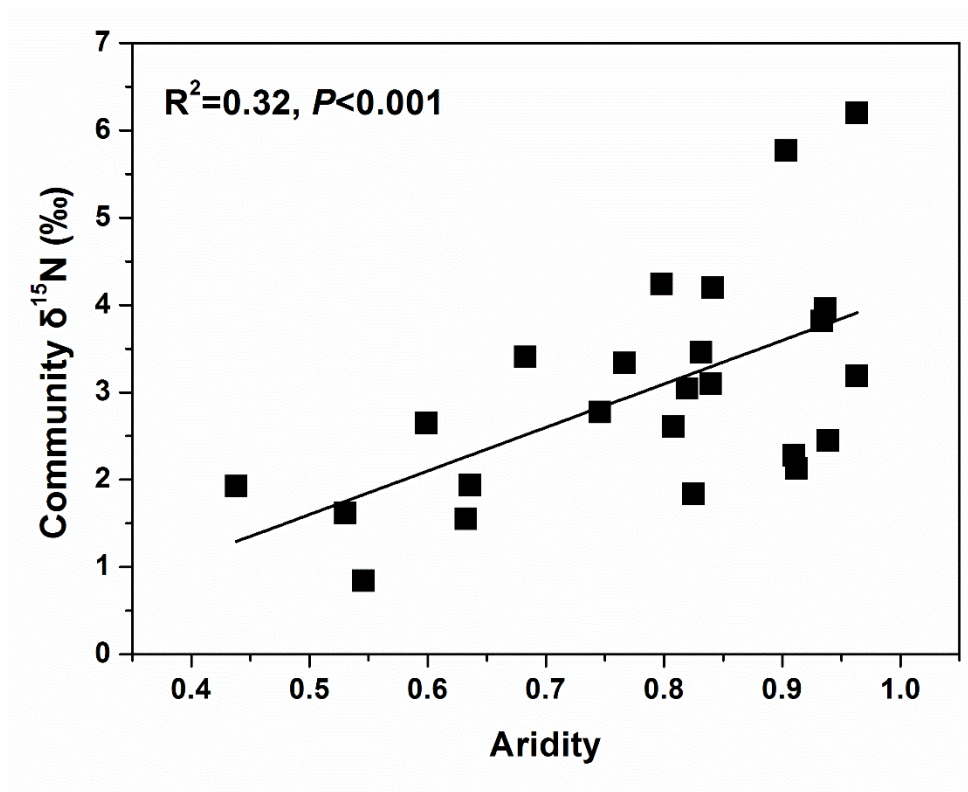
549 **Figure 5** Diagram of the structural equation modeling (SEM) that best explain the
550 maximum variance of (a) C3 and (b) C4 plant N isotopic signatures ($\delta^{15}\text{N}$) along the
551 environmental gradient in northern China. Numbers adjacent to arrows are
552 standardized path coefficients, analogous to relative regression weights, and indicative
553 of the effect size of the relationship. Dashed and continuous arrows indicate negative
554 and positive relationships, respectively. Arrow width is proportional to the strength of
555 the relationship. Goodness-of-fit statistic for each model are shown in the lower right
556 corner. The proportion of variance explained (R^2) appears alongside every response
557 variable in the model. * $P < 0.05$, ** $P < 0.01$, *** $P < 0.001$. Aridity was calculated as 1-
558 AI, where AI, the ratio of precipitation to potential evapotranspiration, is the aridity
559



560

561 **Figure 1**

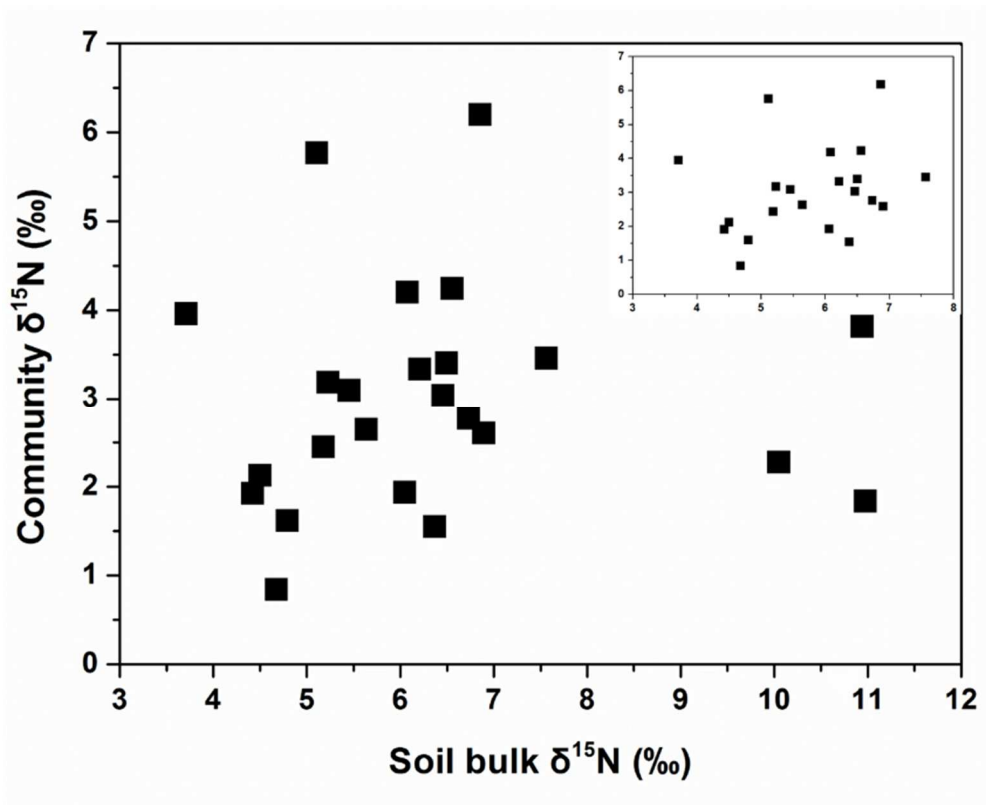
562



563

564 **Figure 2**

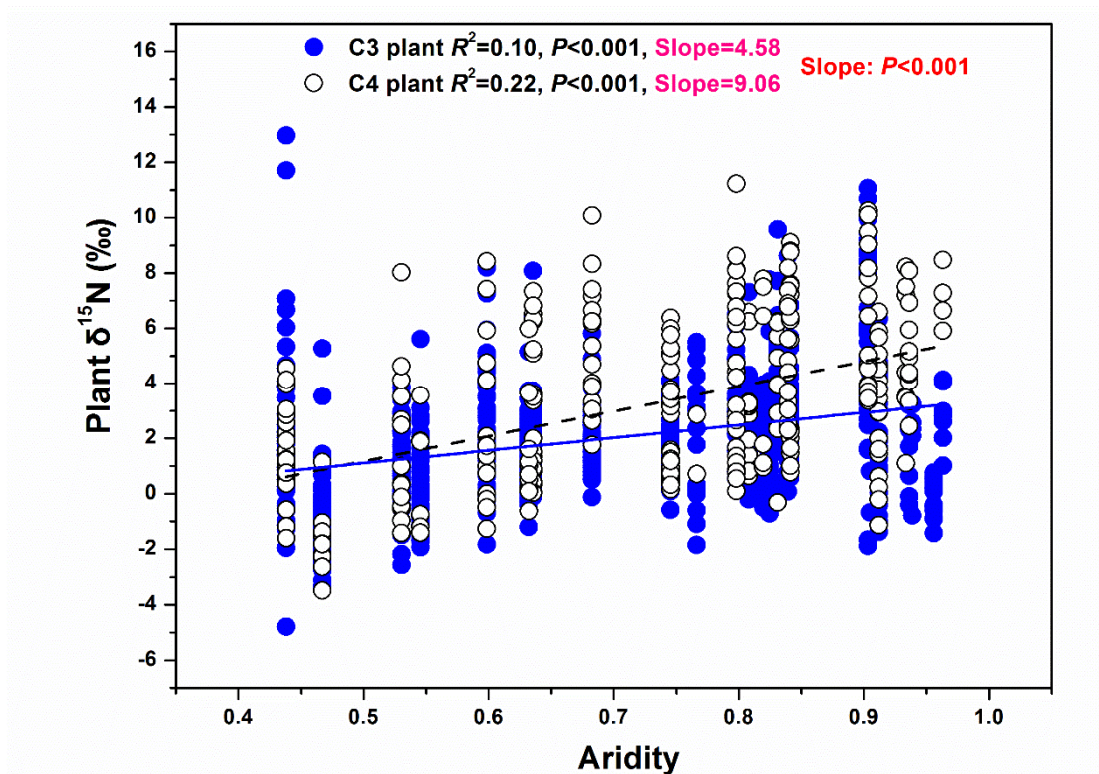
565



566

567 **Figure 3**

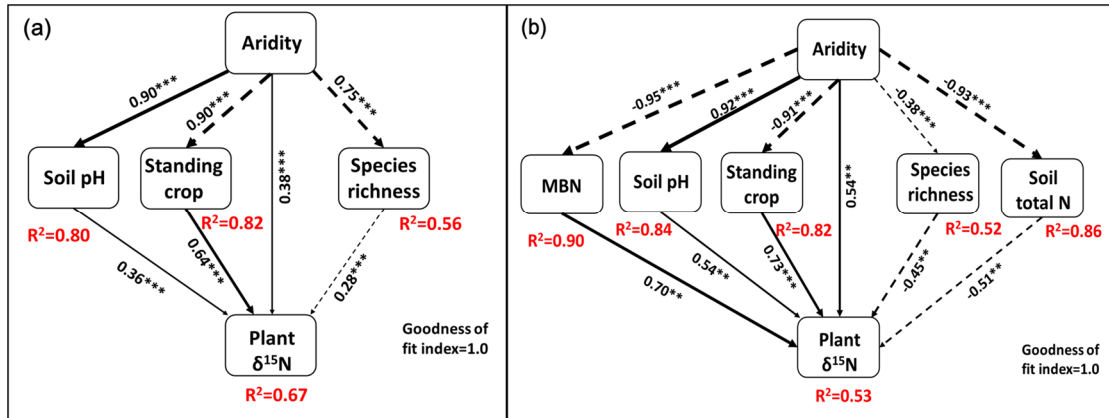
568



569

570 **Figure 4**

571



572

573 **Figure 5**